

Activation Energy for the Emission of 420 nm Luminescence from UV-Excited Polycrystalline H₂O Ice

T. I. Quickenden* and A. R. Hanlon

Department of Chemistry, The University of Western Australia, Nedlands, WA 6907, Australia

C. G. Freeman

Department of Chemistry, University of Canterbury, Christchurch 1, New Zealand

Received: February 18, 1997; In Final Form: April 15, 1997[⊗]

Temperature dependence measurements between 78 and 180 K were carried out on the decay of the 420 nm luminescence emitted by purified polycrystalline H₂O ice, irradiated at 260 nm. Previous work at 78 K showed that a biexponential decay model fitted that luminescence decay quite well. This was also found to be the case at all of the temperatures studied in the present work, the mean lifetimes of the two decays being 0.8 ± 0.1 s and 2.5 ± 0.4 s. Activation energies were found to be negligible in both cases, being less than the experimental error of 0.003 eV. Such low values are consistent with the rate-limiting step being a light-emitting electronic transition rather than a chemical or diffusional step. The 420 nm luminescence is attributed to the spin forbidden $^4\Sigma^- \rightarrow X^2\Pi$ transition of OH radicals from their excited state back to the ground state.

Introduction

Although luminescence from UV-excited ice has been known for some years,^{1–6} very recent work⁷ has focused attention on the $^4\Sigma^- \rightarrow X^2\Pi$ transition of excited OH as the probable emitter of the long-lived 420 nm component of the emission. The choice of the quartet state of OH rather than the ubiquitous $A^2\Sigma^+$ state of OH is surprising at first sight, as the quartet state is probably dissociative⁸ in the gas phase and is presumably⁷ made associative in the solid state.

The $^4\Sigma^- \rightarrow X^2\Pi$ transition is spin forbidden and therefore has the possibility of accounting for the rather long (several seconds) lifetime of the 420 nm emission band studied in the present work. Previous work from this group⁷ has already established that at 78 K, the rise and fall of this luminescence are identical, and this observation is consistent with exponential behavior (as expected for rate-limiting electronic transitions).

If indeed the luminescence is rate-limited by a slow electronic transition, the activation energy of the emission should be negligible because of the absence of temperature dependence in the Einstein coefficient for electronic transition probabilities. The aim of the present paper was to determine the activation energy of the 420 nm emission in order to test this point.

Experimental Section

The equipment and procedures used for the measurement of UV-excited ice luminescence, and the detailed water purification method used, have been fully described previously.⁷ However, in the present study, polycrystalline ice was deposited instead of amorphous ice. Polycrystalline ice samples of ca. 1.5 mm thickness were prepared by spraying a stream of water vapor onto the surface of a high-purity copper substrate at 78 ± 1 K, in a vacuum chamber at ca. 10^{-5} Torr. The rate of deposition (1.4×10^{22} molecules h⁻¹) was controlled by means of a variable leak valve (Granville Phillips Series 203) and was approximately 300 times faster⁹ than the maximum deposition rate which is allowable for amorphous ice formation. There is thus no doubt that the ice samples comprised polycrystalline ice.

The temperature of the ice sample was monitored with a chromel–alumel thermocouple situated directly behind the copper deposition surface. Temperature control was achieved via two electric cartridge heaters situated within the copper sample assembly. These heaters were connected to a temperature controller containing a thermocouple amplifier with cold junction compensation (Analog Devices 595 chip), allowing the temperature to be controlled to within ± 1 K.

All errors quoted in this study are 95% confidence intervals.

Results and Discussion

Problems of Luminescence Drift. One of the unsolved problems associated with UV-excited ice luminescence studies has been the slow increase of luminescence intensity with time. This increase occurs without the need for any significant irradiation of the ice. As this intensity drift is relatively slow, it does not pose a great problem in short-term experiments. Nevertheless, to provide some guidance as to how long kinetic and spectral experiments could be carried out without making significant corrections for drift, a series of replicate intensity drift experiments were carried out over periods of ca. 7 h. The results, shown in Figure 1, illustrate the wide range of intensity–time behaviors for replicate ice samples at 78 K (Figure 1a). Figure 1b shows the rather narrower range of behaviors at the higher temperature of 150 K. It is clear from these two figures that despite a good deal of sample variability, the intensity generally increases quite steeply over the first 2 h and then changes more slowly thereafter but does not reach an obvious plateau. Furthermore, the initial intensity varies significantly from sample to sample, and occasionally the long-term intensity actually decreases with time.

The cause of the drift in luminescence intensity is not known with any degree of certainty, but it is possible that it arises from morphology changes which occur spontaneously on the ice surface over a period of time. Such changes are now well-known and involve dendritic growth¹⁰ on the ice surface, following suspension of the ice in a vacuum. Such growth is now well-established and has been imaged by electron microscopic techniques.¹⁰

It is not entirely clear how the extent of dendritic growth would affect the emission of light from the ice surface.

[⊗] Abstract published in *Advance ACS Abstracts*, June 1, 1997.

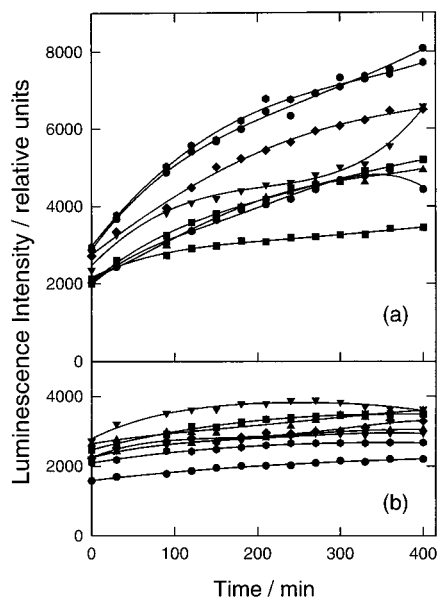


Figure 1. Results of experiments showing the drift of the 420 nm luminescence intensity with time for eight individual polycrystalline ice samples. The ice samples were irradiated only during luminescence measurements with 260 nm UV light. (a) Temperature = 78 K. (b) Temperature = 150 K. The ice samples used in (a) and (b) were deposited at 78 K. The samples used in (b) were then warmed to 150 K before irradiation was commenced, and zero time was taken to be the time when the sample temperature reached 150 K. The ice sample was then held at this temperature (within ± 1 K) for the 400 min duration of the run.

However, in general terms, an increase in the surface area of the ice could increase the emission until shadowing of the surface by the dendrites might cause the increase in emission intensity to reach a plateau level. Any such level does not appear to have been reached in the time period of ca. 7 h used in parts a and b of Figure 1.

Further work will be carried out on the intensity drift and will be the subject of a later paper. However, the purpose of the present investigation of the drift was merely to obtain enough observations to enable temperature dependence experiments to be planned in a manner which prevented the incursion of significant errors from this cause.

In view of the above results, the following strategies for experimental design were adopted. First, Arrhenius analyses of temperature dependence were carried out on luminescence decay rate constants, rather than on luminescence intensities, to avoid the substantial drift problems associated with the use of the latter. Second, a period of 2 h was allowed to elapse after the ice sample had been deposited and before kinetic measurements were taken. With these procedures in place, the maximum percentage change in intensity during any single rise or decay measurement (maximum duration = 30 s) would be a trivial 0.1%.

Spectral Changes as a Function of Temperature. The three-dimensional presentation in Figure 2 shows the change in spectral shape with temperature. Because of the time (20 min) taken to scan each low-intensity spectrum at each temperature, the intensity drifts referred to in the previous section could produce uncertainties of up to 4% in the luminescence intensity ordinate. These are much greater errors than those produced in the decay rate constants but are not of great importance as the main purpose of the intensity spectrum was to provide confirmation that the emission band observed at 420 nm at 78 K remained at this wavelength over the whole temperature range studied.

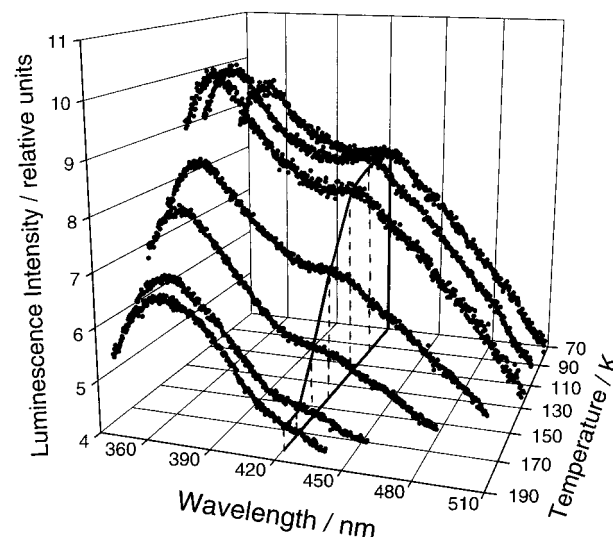


Figure 2. Three-dimensional representation showing the effect of temperature on the luminescence intensity spectra from polycrystalline ice irradiated with 260 nm light. Each spectrum is the mean of three scans, each obtained from a separate ice sample. The emission and excitation monochromators had band passes of 20 nm. A two-dimensional cross section at 420 nm (the wavelength at which kinetic studies were carried out) is shown by the dashed lines, and the 420 nm emission intensities at each temperature are connected by a solid line. All spectra have been corrected for the wavelength responses of the photomultiplier tube, the monochromators, and the borosilicate glass filter.

All of the kinetic measurements in this paper were carried out at 420 nm. The peak located at 420 nm in Figure 2 clearly shows a steep fall in intensity as the temperature is increased beyond 125 K, and the intensity clearly reaches a basal level around 170 K. Importantly, the 420 nm cross section in Figure 2 shows that the decrease in intensity of the 420 nm luminescence with increasing temperature results only from the decrease in peak height, rather than being due to a temperature-induced spectral shift. It should be noted that the character of the luminescence spectrum has changed greatly at temperatures of 200 K and above. The luminescence peak at 420 nm has vanished and the 350 nm peak has apparently moved to 380 nm at 200 K.

Dependence of Luminescence Intensity on the Irradiance of the Exciting Light. The first part of the kinetic study involved determining the effect of incident light irradiance on the luminescence intensity. The background theory associated with such measurements has been detailed previously by Vernon et al.¹¹ for electron-excited ice luminescence. Basically, for a first-order reaction, a plot of $\ln I$ versus $\ln D$ should have a slope of unity, where I is the intensity of the luminescence and D is the irradiance of the exciting light. In the first-order case, this slope should be independent of the time when the irradiances and intensities were measured during the luminescence decay.

Vernon et al.¹¹ also present expressions for the slopes of such plots when second-order reactions with equal reactant concentrations and second-order reactions with unequal reactant concentrations are involved. In the first case the slope, at time t after the commencement of the reaction, is given by the equation¹²

$$d(\ln I)/d(\ln D) = 2/(1 + k_2[A]_0 t) \quad (1)$$

where k_2 is the second-order rate constant, and $[A]_0$ is the initial concentration of reactant A (which is of course equal to $[B]_0$, the initial concentration of reactant B).

TABLE 1: Summary of the Measured Reaction Orders, $d(\ln I)/d(\ln D)$, for the 420 nm Luminescence over the Temperature Range 78–180 K^a

temperature, K	$d(\ln I)/d(\ln D)$	temperature, K	$d(\ln I)/d(\ln D)$
78	1.04 ± 0.23	140	1.04 ± 0.10
90	1.00 ± 0.01	155	1.04 ± 0.27
110	0.99 ± 0.11	170	1.03 ± 0.01
125	1.10 ± 0.19	180	1.11 ± 0.25

^a I is equal to the luminescence intensity, and D is the irradiance of the exciting UV light. Values of $d(\ln I)/d(\ln D)$, at each temperature, were obtained from four replicate measurements on each of three freshly prepared ice samples, with the errors representing 95% confidence intervals. Total errors in the temperature (including both systematic and random errors) are believed to be no more than ± 1 K.

For the second-order with unequal concentration model, the slope is given by¹¹

$$d(\ln I)/d(\ln D) = 2 + \{(k_2 t [A]_0 (1 - R)(R + e^{\omega t}) / (R - e^{\omega t}))\} \quad (2)$$

where $R = [B]_0/[A]_0$ and $\omega = k_2[A]_0(1 - R)$.

In both second-order cases, the slope of an $\ln I$ versus $\ln D$ plot is 2 at early times after the start of the luminescence decay. As the irradiance dependence measurements were carried out at a constant light irradiance (before any shuttering of the exciting light had been carried out), these measurements are effectively zero-time measurements, and thus slopes of 2 would have been obtained if the decays followed second-order or second-order unequal kinetics.

Table 1 shows the values of $d(\ln I)/d(\ln D)$ observed for the 420 nm luminescence in the present study. It is clear that all the values lie within experimental error of unity, thus providing strong support for the rate-limiting step being a first-order process or a set of parallel first-order processes.

Luminescence Decay Kinetics. Luminescence decay curves were obtained by manually shuttering the incident UV light source and recording the resulting fall in luminescence intensity over time on a digital storage oscilloscope (Thurlby DSA 542). Five luminescence decay curves were obtained at each temperature. The temperature was progressively raised through eight values, from 78 to 180 K, by warming the sample assembly by passing current through the cartridge heaters, as described in the Experimental Section. The ice was held at each temperature for ca. 20 min while the five replicate decay experiments were carried out. This process was repeated on different days on eight different ice samples. The whole process was repeated at a later time at another seven different temperatures (chosen to fall between the previous eight temperatures) on another eight freshly prepared ice samples. Luminescence rise curves were also obtained using the same procedure as above, except that the shutter was rapidly opened (instead of closed) thereby irradiating the ice sample with exciting light, the resulting rise in luminescence intensity again being recorded on the digital oscilloscope.

At each temperature, the replicate decay curves were normalized to the same initial luminescence intensities before the mean decay curve was calculated. The replicate rise curves for each temperature were normalized in the following way. First, the luminescence intensities 0.5 s after shuttering were moved vertically down to zero intensity. Second, each curve was multiplied by a factor which ensured that the final plateau intensities were all the same. Third, these normalized rise curves were all meaned.

Considerable detail has been given in previous papers from this group^{7,11} on the fitting of kinetic models to luminescence

decay curves. The curve-fitting procedure was carried out on the 0.5–12 s portion of the curves. All the kinetic models listed in our recent paper⁷ were fitted to the mean luminescence decays using the procedures set out therein. As usual,⁷ the criteria for best fit were taken to be minimum values for the sums of the squares of the residuals (SSR) and minimal correlation in residuals plots. The biexponential model was found to provide the best fit over the full temperature range, with the second-order with unequal reactant concentration model and the model described by Plonka¹³ giving slightly higher SSR values, especially at the lower temperatures. However, at the higher temperatures, the three models gave very similar SSR values, and therefore the second-order unequal and Plonka models could not be ruled out on the basis of the SSR alone.

The biexponential model expresses the luminescence intensity as the sum of two single-exponential decays, viz.:

$$I = ae^{-k_a t} + be^{-k_b t} \quad (3)$$

where I is the luminescence intensity at time t , a and b are constants that describe the initial intensities of the two first-order decays that comprise the biexponential decay, and k_a and k_b are the first-order rate constants for the two parallel luminescence decays.

The second-order with unequal reactant concentrations model assumes that the luminescent species arises from the combination of two homogeneously distributed photolysis products (A and B). These reactants are not in equal concentrations. The equation is

$$I = k_2 [A]_0^2 R \omega e^{\omega t} (1 - R) / (R - e^{\omega t})^2 \quad (4)$$

where k_2 , R , $[A]_0$, and ω were defined when eq 2 was presented.

The model described by Plonka¹³ contains a time-dependent rate constant and is derived by summing a large number of competing exponential decays. The equation derived by Plonka is

$$I = \gamma \alpha \tau_0^{-1} (t/\tau_0)^{\alpha-1} \exp[-(t/\tau_0)^\alpha] \quad (5)$$

where γ is a preexponential factor, α has a value between 0 and 1, and τ_0 is referred to as the “effective lifetime”.

Other kinetic models⁷ such as a single-exponential model, second-order decay with equal reactant concentrations, and those of tunneling and fractal kinetics gave very poor fits to the decay data. However, the three models expressed by eqs 3 to 5 fitted the luminescence decay curves very well. However, as the measurements of the effect of irradiance on the luminescence emission intensity showed that the reaction order for the rate-limiting step was unity (Table 1), the second-order with unequal concentrations option is ruled out.

Quickenden et al.⁷ have shown that in amorphous ice at 78 K, the luminescence rise and decay are essentially mirror images of one another. In this present study on polycrystalline ice, the luminescence rise and decay were compared at temperatures between 78 and 180 K. As found for the 78 K temperature in the previous study,⁷ the rise and fall times were identical, within experimental error, over the whole temperature range. Figure 3 shows that if the luminescence rise data is inverted, the resulting curve may be superimposed on the luminescence decay data, illustrating the identical rise and fall times. The rise curves were transformed by plotting the difference between the final (plateau) intensity (I_f) and the luminescence intensity at a given time during the rise (I_t), as a function of time t (i.e. $I_f - I_t$ versus t), and normalizing the inverted rise curve to the same initial intensity as the corresponding decay curve. Points on the

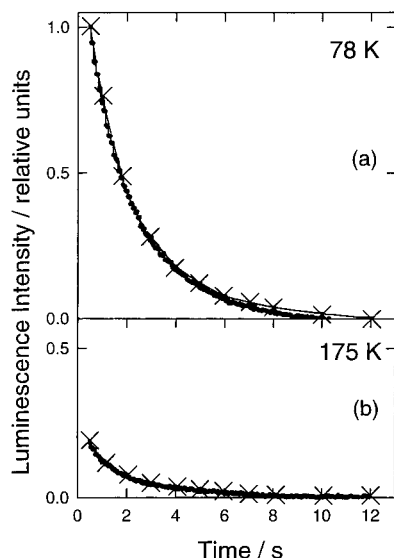


Figure 3. Comparison of the decay (point symbols) of the 420 nm luminescence from UV-irradiated polycrystalline ice with the rise of the luminescence (crosses joined by a solid line) after the latter had been inverted by a transformation described in the text. (a) Temperature = 78 K. (b) Temperature = 175 K. The rise and fall curves are each the mean of 40 replicate measurements comprising five replicates on each of eight freshly prepared ice samples.

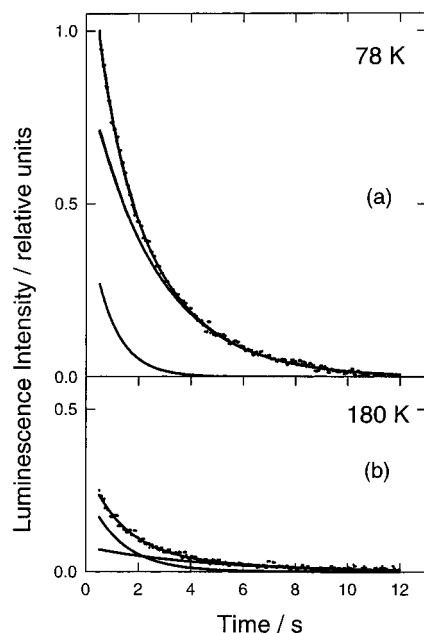


Figure 4. The biexponential fit to the mean 420 nm ice luminescence decay data is shown as a solid line passing through the point symbols. (a) Temperature = 78 K. (b) Temperature = 180 K. The separate contributions of the two first-order decays which comprise the overall decay are also shown. The decay data were obtained as the means of 40 replicate measurements comprising five replicates on each of eight freshly prepared ice samples. Excitation and emission band passes were 20 nm. The curve-fitting procedure was carried out on the 0.5–12 s portion of the decay curves.

transformed rise curve are represented by crosses and the dots represent the decay data. Quickenden et al.⁷ have shown that such behavior is consistent with exponential or biexponential models. This behavior is not consistent with the second-order (unequal reactant concentrations) model (eq 4) and nor is it likely to be consistent with the more complex Plonka model (eq 5).

Figure 4 shows the mean luminescence decay curve data at the lowest and highest temperatures of 78 and 180 K, respec-

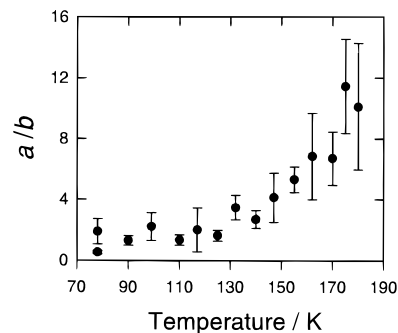


Figure 5. Plot of the ratio a/b as a function of temperature, where a is the initial intensity (at 0.5 s) of the short-lived component of the luminescence decay, and b is the initial intensity of the longer-lived component. Error bars represent 95% confidence intervals. Where error bars cannot be seen, they are smaller than the point size.

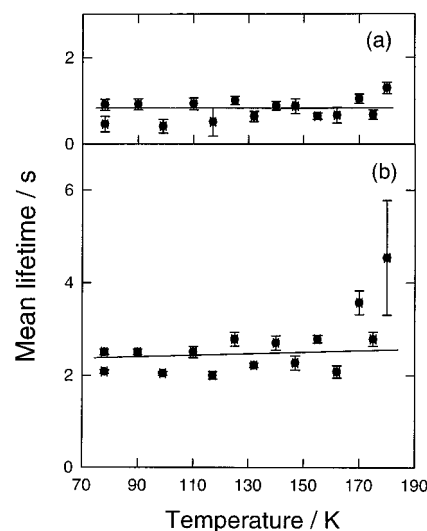


Figure 6. Plot of the mean lifetime ($1/k$) as a function of temperature, for (a) the short-lived 420 nm ice luminescence decay and (b) the longer-lived decay. Error bars represent 95% confidence intervals. Where error bars cannot be seen, they are smaller than the point size.

tively. It is clear that the biexponential model fits the experimental data well at these two temperatures. The data for intermediate temperatures is not shown, but similarly good fits were obtained. Figure 4 also shows (underneath the total decay curve data) the separate contributions from the two individual first-order decays which constitute the biexponential decay curve. As the ice temperature is raised, the luminescence decay curves decrease in starting intensity, the two contributing exponential decays (the short- and longer-lived) decreasing by different amounts. Figure 5 shows that the ratio of the initial luminescence intensities (at 0.5 s), a/b , increases with increasing temperature. This change in ratio was largely due to the decrease in b with increasing temperature, while a remained fairly constant over the whole temperature range studied.

Parts a and b of Figure 6 show how the mean lifetimes of the short- (a) and longer-lived (b) components of the luminescence decay vary very little with temperature. The mean lifetime was calculated as the inverse of the rate constants determined from the biexponential fit (ie. $1/k_a$ for Figure 6a and $1/k_b$ for Figure 6b). The lifetime remains fairly constant over the full temperature range, averaging 0.8 ± 0.1 s for the short-lived decay, and 2.5 ± 0.4 s for the longer-lived decay. It can be seen from Figure 6b, that at the highest temperature the lifetime of the longer-lived decay may be increasing, but it has a very large error.

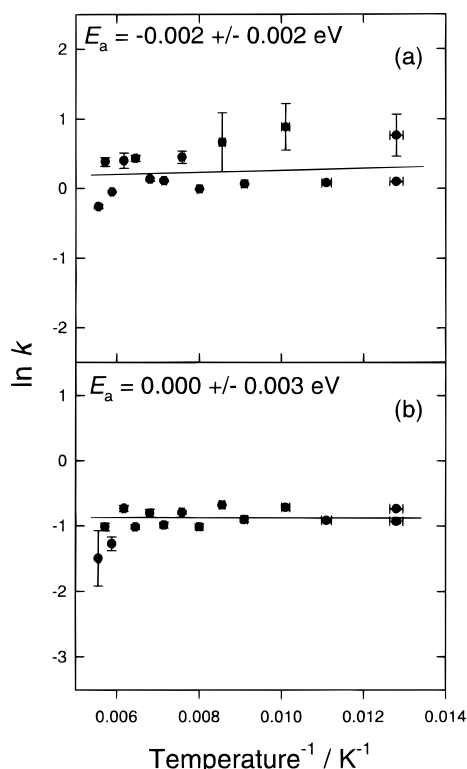


Figure 7. The Arrhenius plots obtained from (a) k_a (the earlier decay) and (b) k_b (the later decay) obtained from the biexponential fits to the 420 nm ice luminescence data. Error bars represent 95% confidence intervals. Where error bars cannot be seen, they are smaller than the point size.

Activation Energy Determination. Activation energies, E_a , were determined from the Arrhenius equation:

$$k = Ae^{-E_a/RT}$$

where k is the rate constant for the luminescence decay, T is the Kelvin temperature, R is the gas constant, and A is the preexponential factor. The activation energies were determined from the slopes of plots of $\ln k$ versus $1/T$.

Figure 7 shows Arrhenius plots for the early exponential decay (rate constant k_a) and the later exponential decay (k_b) obtained from the biexponential fits. The early decay data is less accurate and contains more random error, whereas the longer-lived decay contains less random error. Nevertheless, both sets of data (Figure 7) give Arrhenius plots which show no significant activation energy, the values of E_a derived from the slopes being smaller than the 95% confidence interval error in both cases.

Table 2 shows a number of literature activation energies that have been determined for various processes in ice. The lowest of these are clearly of greater relevance to the present work because of the very low slopes obtained from the present Arrhenius plots. However, even the lowest activation energies in Table 2 (those for the diffusion of H⁺ in ice) are higher by a factor of about 10 times than the 95% confidence interval errors attached to the zero activation energies found in the present work. It is thus clear that some very low activation energy process (even lower than for H⁺ diffusion through the ice lattice) must be the rate-limiting step for the production of the 420 nm luminescence.

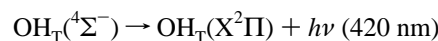
Such a small temperature dependence would be expected if the rate-limiting step was simply an electronic transition, as zero temperature dependence is contained in the Einstein expression for electronic transition probabilities. Quickenden et al.,⁷ have

TABLE 2: A Selection of Literature Values of Low Activation Energies (E_a), for the Decays and Mobilities of Species That Have Been Detected in Irradiated Ice

species	process	E_a /eV	temp, K	authors
H	decay	ca. 0.043–0.11	30–50	Flournoy et al. ^b
H	decay	ca. 0.086	77–87	Plonka et al. ^c
H ⁺	mobility ^a	0.021	96–106	Eckener et al. ^d
H ⁺	mobility ^a	0.041	108–118	Eckener et al. ^d
e ⁻	decay	0.1–0.2	77–130	Warman et al. ^e
OH	decay	0.26 ± 0.02	92–107	Siegel et al. ^f
OH	decay	0.06	77–200	Maria and McGlynn ^g
luminescence decay (fast)		-0.002 ± 0.002	78–180	present study
luminescence decay (slow)		0.000 ± 0.003	78–180	present study

^a The Arrhenius plots that gave these values were obtained using the temperature dependences of the mobilities of the species, while the other activation energies were determined from the temperature dependences of their decay rates. ^b Reference 14. ^c Reference 15. ^d Reference 16. ^e Reference 17. ^f Reference 18. ^g Reference 19. Errors in the present study represent 95% confidence intervals.

recently proposed that the rate-limiting step for the 420 nm luminescence is a particular electronic transition, namely the transition from the quartet state of excited OH down to its ground state viz.



The biexponentiality of the luminescence decay was attributed by Quickenden et al.⁷ to the OH radicals occupying two distinct environments within the ice lattice, viz. substitutional and interstitial sites.^{20,5} Slight differences in the local environment of each trapping site could perturb the transition probability differently and hence produce the two different decay rates. The much greater decrease of the longer-lived luminescence compared with that of the short-lived luminescence with increasing temperature could arise because increasing the temperature has altered the relative concentrations of the substitutional and interstitial trapping sites in the ice. Ghormley and Hochanadel²⁰ propose that at temperatures in excess of about 123 K, OH radicals become trapped predominantly in substitutional sites, whereas at lower temperatures, the OH is trapped mainly in interstitial trapping sites. It is also possible that the increase in temperature has affected the relative occupancies of these sites by OH radicals or has altered the relative transition probabilities of the excited OH radicals therein. Further studies will be necessary to determine which of these is the most likely option.

Conclusions

Although increasing the temperature of UV-irradiated ice significantly decreases the intensity of the 420 nm luminescence peak, the rate constants for the luminescence decays associated with this peak are not significantly affected. This indicates that the rate-limiting step of the processes which occur after the exciting light is shuttered has negligible activation energy and is thus the electronic transition for light emission. This result provides further evidence for the previous assignment of the luminescence to the $^4\Sigma^- \rightarrow X^2\Pi$ transition of excited OH radicals.

References and Notes

- (1) Vierke, G.; Stauff, J. *Ber Bunsen-Ges. Phys. Chem.* **1970**, *74*, 358.
- (2) Quickenden, T. I.; Litjens, R. A. J.; Freeman, C. G.; Trotman, S. M. *Chem. Phys. Lett.* **1985**, *114*, 164.
- (3) Litjens, R. A. J.; Quickenden, T. I. *J. Phys. (Paris) Colloid Cl.* **1987**, *48*, 59.
- (4) Lennon, D.; Quickenden, T. I.; Freeman, C. G. *Chem. Phys. Lett.* **1993**, *201*, 120.
- (5) Matich, A. J.; Bakker, M. G.; Lennon, D.; Quickenden, T. I.; Freeman, C. G. *J. Phys. Chem.* **1993**, *97*, 10539.

- (6) Matich, A. J. Luminescence from Ultraviolet and Electron Irradiated Ice. Ph.D. Thesis, The University of Western Australia, Perth, Australia, 1992.
- (7) Quickenden, T. I.; Green, T. A.; Lennon, D. *J. Phys. Chem.* **1996**, *100*, 16801.
- (8) Mathers, T. L.; Nauman, R. V.; McGlynn, S. P. *Chem. Phys. Lett.* **1986**, *126*, 408.
- (9) Sivakumar, T. C.; Rice, S. A.; Sceats, M. G. *J. Chem. Phys.* **1978**, *69*, 3468.
- (10) Cross, J. D. *Science* **1969**, *64*, 174.
- (11) Vernon, C. F.; Matich, A. J.; Quickenden, T. I.; Sangster, D. F. *J. Phys. Chem.* **1991**, *95*, 7313.
- (12) Trotman, S. M.; Quickenden, T. I.; Sangster, D. F. *J. Chem. Phys.* **1986**, *85*, 2555.
- (13) Plonka, A. *Annu. Rep. Prog. Chem., Sect. C* **1988**, *85*, 60.
- (14) Flournoy, J. M.; Baum, L. H.; Siegel, S. *J. Chem. Phys.* **1962**, *36*, 2229.
- (15) Plonka, A.; Kroh, J.; Lefik, W.; Bogus, W. *J. Phys. Chem.* **1979**, *83*, 1807.
- (16) Eckener, U.; Helmreich, D. Engelhardt, H. in *Physics and Chemistry of Ice*, edited by Whalley, E.; Jones, S. J.; Gold, L. W.; Royal Society of Canada, Ottawa, 1973.
- (17) Warman, J. M.; de Haas, M. P.; Verberne, J. B. *J. Phys. Chem.* **1980**, *84*, 1240.
- (18) Siegel, S.; Baum, L. H.; Skolnik, S.; Flournoy, J. M. *J. Chem. Phys.* **1960**, *32*, 1249.
- (19) Maria, H. J.; McGlynn, S. P. *J. Chem. Phys.* **1970**, *52*, 3402.
- (20) Ghormley, J. A.; Hochanadel, C. J. *J. Phys. Chem.* **1971**, *75*, 40.